4-15-2016

Input space-dependent controller for multi-hazard mitigation

Liang Cao
Iowa State University

Simon Laflamme
Iowa State University, laflamme@iastate.edu

Input space-dependent controller for multi-hazard mitigation

Abstract
Semi-active and active structural control systems are advanced mechanical devices and systems capable of high damping performance, ideal for mitigation of multi-hazards. The implementation of these devices within structural systems is still in its infancy, because of the complexity in designing a robust closed-loop control system that can ensure reliable and high mitigation performance. Particular challenges in designing a controller for multi-hazard mitigation include: 1) very large uncertainties on dynamic parameters and unknown excitations; 2) limited measurements with probabilities of sensor failure; 3) immediate performance requirements; and 4) unavailable sets of input-output during design. To facilitate the implementation of structural control systems, a new type of controllers with high adaptive capabilities is proposed. It is based on real-time identification of an embedding that represents the essential dynamics found in the input space, or in the sensors measurements. This type of controller is termed input-space dependent controllers (ISDC). In this paper, the principle of ISDC is presented, their stability and performance derived analytically for the case of harmonic inputs, and their performance demonstrated in the case of different types of hazards. Results show the promise of this new type of controller at mitigating multi-hazards by 1) relying on local and limited sensors only; 2) not requiring prior evaluation or training; and 3) adapting to systems non-stationarities.

Keywords
input-space dependent controller, time delay controller, embedding theorem, multi-delay, multi-hazard, structural control

Disciplines
Civil Engineering | Construction Engineering and Management | Controls and Control Theory | VLSI and Circuits, Embedded and Hardware Systems

Comments
This proceeding is published as Liang Cao, Simon Laflamme, "Input space-dependent controller for multi-hazard mitigation", Proc. SPIE 9799, Active and Passive Smart Structures and Integrated Systems 2016, 97992H (15 April 2016); doi: 10.1117/12.2219263. Posted with permission.

Input Space-Dependent Controller for Multi-Hazard Mitigation

Liang Cao[a] and Simon Laflamme[a,b]

[a]Department of Civil, Construction, and Environmental Engineering, Iowa State University, Ames, IA 50011, USA
[b]Department of Electrical and Computer Engineering, Iowa State University, Ames, IA 50011, USA

ABSTRACT

Semi-active and active structural control systems are advanced mechanical devices and systems capable of high damping performance, ideal for mitigation of multi-hazards. The implementation of these devices within structural systems is still in its infancy, because of the complexity in designing a robust closed-loop control system that can ensure reliable and high mitigation performance. Particular challenges in designing a controller for multi-hazard mitigation include: 1) very large uncertainties on dynamic parameters and unknown excitations; 2) limited measurements with probabilities of sensor failure; 3) immediate performance requirements; and 4) unavailable sets of input-output during design. To facilitate the implementation of structural control systems, a new type of controllers with high adaptive capabilities is proposed. It is based on real-time identification of an embedding that represents the essential dynamics found in the input space, or in the sensors measurements. This type of controller is termed input-space dependent controllers (ISDC). In this paper, the principle of ISDC is presented, their stability and performance derived analytically for the case of harmonic inputs, and their performance demonstrated in the case of different types of hazards. Results show the promise of this new type of controller at mitigating multi-hazards by 1) relying on local and limited sensors only; 2) not requiring prior evaluation or training; and 3) adapting to systems nonstationarities.

Keywords: input-space dependent controller, time delay controller, embedding theorem, multi-delay, multi-hazard, structural control

1. INTRODUCTION

Semi-active and active structural control systems[1–3] have gained popularity in the field of structural control. Compared with passive systems, they are typically capable of substantially better mitigation performance over a larger excitation bandwidth.[4–6] However, these devices are not widely accepted due to applicability obstacles over the entire control loop. In particular, designing a robust controller for civil structures is challenging, because: 1) uncertainties on dynamic parameters are very large, and excitations are unknown and varying in the case of a multi-hazard framework; 2) available measurements are limited and sensors have non-negligible probabilities of failure over time; 3) there is an immediate performance requirements; and 4) input-output data sets are unavailable.[7,8]

There has been much work in designing controllers tailored to the structural control challenge. Model-driven controllers (MDCs), including linear quadratic regulators and Lyapunov controllers, have shown great potential, but require some level of knowledge of the system to be controlled. MDCs may not perform well in the presence of model inaccuracies.[9,10] A solution is data-driven controllers (DDCs), which rely on implicit information from past and present measurements.[11] While these controllers are designed to cope with systems' unknowns and uncertainties, they may underperform MDCs because they overlook physical knowledge of the system. DDCs include neurocontrollers,[12–14] model-free adaptive controllers,[15] SPSA-based data driven control (SPSA),[16] unfalsified control (UC),[17] virtual reference feedback tuning (VRFT),[18] and fuzzy controllers.[19]

Of particular interest are DDCs based on time delay observation feedback in the form

Further author information: (Send correspondence to Liang Cao)
Liang Cao: E-mail: liangcao@iastate.edu, Telephone: 1 716 472 6595

Active and Passive Smart Structures and Integrated Systems 2016, edited by Gyuhae Park, Proc. of SPIE
Vol. 9799, 97992H · © 2016 SPIE · CCC code: 0277-786X/16/$18 · doi: 10.1117/12.2219263

$$u(t) = \sum_{i=1}^{d} k_i y(t-(i-1)\tau) = \mathbf{K}^T \nu \tag{1}$$

where u is the control force varying as a function of time t, y is an observation or input, k and $\mathbf{K} \in \mathbb{R}^{d\times 1}$ are the control gain and the control gain matrix, respectively, d is the number of delays, τ is the time delay, and $\nu \in \mathbb{R}^{d\times 1}$ is the delay vector. These controllers are designed to provide control decisions based on limited and local measurements. In related work, Pyragas proposed the time-delay autosynchronization (TDAS) method to stabilize the response of chaotic systems.[20] The TDAS is design to stabilize the system by changing the Lyapunov exponents of unstable periodic orbits. The method found limitations in the high period orbits. Instead, Socolar, Sukow and Gauthier[21] proposed a generalization of TDAS controllers, the extended TDAS (ETDAS), which applies to systems with large Lyapunov exponents and high period unstable period orbits. The ETDAS showed limitations in controlling unstable steady states. Ahlborn and Parlitz[22] proposed a multiple delay feedback control (MDFC) to overcome the limitations of both TDAS and ETDAS. The MDFC includes two or more delayed feedback signals with different time delays. The MDFC showed good improvement in performance, but introduced a significant numbers of control parameters.[23] Gjurchinovski and Urumov proposed a variable delay feedback control (VDFC)[24] to improve the performance of TDAS in controlling unstable steady state. The time delay is modulated during the control process, where $\tau = \tau(t)$ in Eq. (1). A limitation of the VDFC is the need to pre-define time delay functions.

A critical limitation of these time delay controllers is the unavailability of online selection rules for τ and d. These parameters are typically selected through tuning. This strategy is difficult to apply in a context where no pre-training or pre-tuning opportunity is available, which is typical for civil structures exposed to multi-hazards. In this paper, we propose the input-space dependent controller (ISDC), with is designed to include automatic selection and adaptation rules for $\tau = \tau(t)$ and $d = d(t)$ based on the topology of the input space. The ISDC can therefore adapt the control rule to different types of excitation inputs.

The selection rule for $\tau(t)$ is based on the Embedding Theorem.[25–27] From this theorem, it can be shown that there exists an optimal delay vector $\nu^*(\tau^*, d^*)$ which contains the essential dynamics of the system, where the asterisk denotes an optimal value. The theorem has been initially developed for autonomous systems,[25] and extended to a general class of nonautonomous systems with deterministic forcing,[26] state-dependant forcing,[28] and stochastic forcing.[27] It has also been shown that ν can be modified to include multivariate observations and unknown inputs.[29] The ISDC seeks τ^* and d^* from the inputs, where the term "input-space dependent", and uses these values to constitute the control rule (Eq. (1)). The Embedding Theorem has been used in several engineering applications, including structural health monitoring[29–31] and structural control.[7,32–35] However, never the online selection of τ and d has been addressed, nor the idea of a time-varying architecture of the delay vector applied. The discussion in this paper is restricted on the selection rule for $\tau(t)$. In what follows, d will be taken as a constant.

This paper is organized as follows. Section 2 studies the optimal time delay provided by the derivation of the analytical solution of a single-degree-of-freedom (SDOF) system, and compares with the optimal time delay from information theory. This comparison will demonstrate the applicability of an embedding theorem-based selection rule. Section 5 presents the ISDC algorithm, which includes the online time delay selection strategy along with adaptive control gains to ensure stability. Section 4 simulates the ISDC under harmonic and impulse loadings to demonstrate the advantages of the controller. Section 5 concludes the paper.

2. OPTIMAL TIME DELAY SELECTION

This section studies the applicability of the Embedding Theorem for selecting τ. Consider an SDOF of the form

$$m\ddot{x}(t) + c\dot{x}(t) + kx(t) = f(t) + u(t) \tag{2}$$

where m, c and k are the system's mass, damping and stiffness, respectively, $f(t)$ is an external excitation, $u(t)$ is the control force from Eq. (1), x is the displacement, and the dot denotes the time derivative. For simplicity, assume that the observation

$y(t) = x(t)$. The Embedding Theorem states that the topological space of the dynamic system can be reconstructed using v^*. Such v^*, constructed with τ^* and d^*, comprises the essential dynamics of the system. Based on this information, it is hypothesized that the utilization of v^* as control input would provide a DDC with sufficient information about the system's dynamics, therefore enabling good control performance.

The upcoming subsection derives the optimal fixed time delay computed using the analytical solution of an SDOF system subjected to a harmonic excitation and controlled with a fixed time delay and constant $d = 2$. A dimension $d = 2$ is selected, as it can be shown to be sufficient to embed a harmonic response.[36] The stability bounds on τ are also determined. The subsequent subsection verifies the hypothesis that v^* could be used as the optimal control input by comparing the analytical solution given by information theory to the analytical solution derived from the SDOF system.

2.1 Optimal Time Delay - SDOF Analytical Solution

Taking the SDOF from Eq. (2) with the following control rule:

$$u(t) = -k_1 x(t) - k_2 x(t-\tau) \tag{3}$$

and using the transformations $\rho_{k1} = k_1/k$ and $\rho_{k2} = k_2/k$ gives:

$$\ddot{x}(t) + 2\xi\omega_n\dot{x}(t) + \omega_n^2 x(t) = -\rho_{k1}\omega_n^2 x(t) - \rho_{k2}\omega_n^2 x(t-\tau) + f(t)/m \tag{4}$$

where $\omega_n = \sqrt{k/m}$ and $\xi = \frac{c}{2m\omega_n}$ are the natural frequency and fundamental damping ratio of system, respectively.

The response of the system represented in Eq. (4) subjected to a harmonic forcing $f(t)$ of the type

$$f(t) = \hat{f}\sin(\Omega t) \tag{5}$$

where $\hat{f}$ and Ω the are the magnitude and frequency of the excitation, respectively, can be expressed in the form

$$x(t) = A\sin(\Omega t) + B\cos(\Omega t) \tag{6}$$

with

$$\begin{cases} -A\Omega^2 - 2\xi\omega_n\Omega B + \omega_n^2 A + \rho_{k1}A + \rho_{k2}(A\cos\tau + B\sin\tau) = \frac{\hat{f}}{m} \\ -B\Omega^2 + 2\xi\omega_n\Omega A + \omega_n^2 B + \rho_{k1}B + \rho_{k2}(B\cos\tau - A\sin\tau) = 0 \end{cases} \tag{7}$$

Solving for A and B in Eq. (7) and substituting back in Eq. (6) yields a transfer function $H = \max(x(t)) \cdot k/\hat{f}$

$$H = \frac{1}{[1-\rho^2+\rho_{k1}+\rho_{k2}\cos(2\pi\rho_\tau)]^2 + [\rho_{k2}\sin(2\pi\rho_\tau) - 2\xi\rho]^2} \tag{8}$$

Fig. 1 is the plot of H versus ρ for various values of ρ_τ, where $\rho = \Omega/\omega_n$ and $\rho_\tau = \tau/T$. The figure is obtained using $\rho_{k1} = 2$ and $\rho_{k2} = -1$, and $\rho_\tau \leq 0.25$, as any additional delay would provide redundant information in terms of topology of the phase-space. Results show that increasing ρ_τ reduces H, until a critical frequency ratio ρ_{cr} is reached. An expression for ρ_{cr} can be obtained by substituting appropriate values for ρ_τ in (8)

$$\rho_{cr} = \xi + \sqrt{\xi^2 + \rho_{k1} + 1} \tag{9}$$

Before concluding on the optimal time delay, a stability analysis is conducted in what follows in order to provide bounds on ρ_τ, ρ_{k1}, and ρ_{k2}.

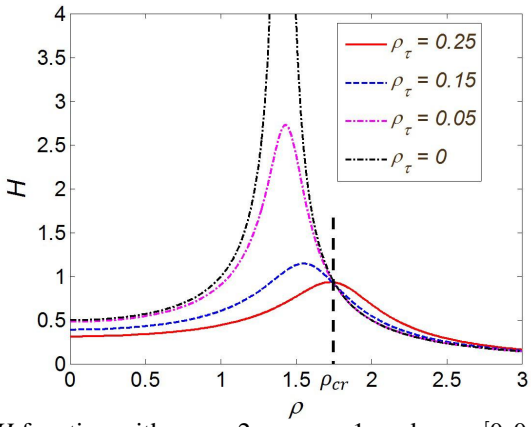

Figure 1: H function with $\rho_{k1} = 2$, $\rho_{k2} = -1$, and $\rho_\tau = [0, 0.05, 0.15, 0.25]$

2.1.1 Stability Analysis

For the stability analysis, the homogeneous solution for $x(t)$ in Eq. (6) is expressed in the form $x(t) = \hat{x}e^{\lambda t}$, where $\hat{x}$ is an amplitude, yielding the characteristic equation

$$\lambda^2 + 2\xi\omega_n\lambda + \omega_n^2 + \rho_{k1}\omega_n^2 + \rho_{k2}\omega_n^2 e^{-\tau\lambda} = 0 \tag{10}$$

The exponential term can be expressed by the power series

$$e^{-\tau\lambda} = 1 - \tau\lambda + \frac{1}{2}(\tau\lambda)^2 - \frac{1}{6}(\tau\lambda)^3 + \ldots \tag{11}$$

Neglecting the higher order terms and retaining the first two terms only, equation (10) becomes

$$\lambda^2 + (2\xi\omega_n - \rho_{k2}\omega_n^2\tau)\lambda + \omega_n^2 + \rho_{k1}\omega_n^2 + \rho_{k2}\omega_n^2 = 0 \tag{12}$$

Here, λ has two complex roots $\lambda_R \pm \lambda_I i$, estimated as

$$\begin{aligned} \lambda_R &= -\xi\omega_n + \frac{1}{2}\rho_{k2}\omega_n^2\tau \\ \lambda_I &= \frac{1}{2}\omega_n\sqrt{4 + 4\rho_{k1} + 4\rho_{k2} - (2\xi - \rho_{k2}\omega_n\tau)^2} \end{aligned} \tag{13}$$

The system is stable if $\lambda_R < 0$, which gives an expression for ρ_{k2}

$$\rho_{k2} < 2\xi/(\omega_n\tau) \tag{14}$$

Furthermore, if λ has two real numbers as roots, the imaginary part vanishes and λ becomes

$$\lambda = -\xi\omega_n + \frac{1}{2}\rho_{k2}\omega_n^2\tau \pm \frac{1}{2}\omega_n\sqrt{4 + 4\rho_{k1} + 4\rho_{k2} - (2\xi - \rho_{k2}\omega_n\tau)^2} \tag{15}$$

The maximum root of λ needs to be negative for $\lambda < 0$, yielding

$$1+\rho_{k1}+\rho_{k2}>0 \tag{16}$$

Eqs. (14) and (16) are stability criterions for control gains k_1 and k_2.

In addition, the exponential term in (10) can be further expanded to study the stability of τ in terms of ρ_{k1} and ρ_{k2}

$$e^{-\tau\lambda}=\frac{1-\frac{1}{2}\tau\lambda}{1+\frac{1}{2}\tau\lambda}+O[(\tau\lambda)^3] \tag{17}$$

which yields a third degree polynomial in λ

$$\tau\lambda^3+(2+2\xi\omega_n\tau)\lambda^2+(4\xi\omega_n+\omega_n^2\tau+\rho_{k1}\omega_n^2\tau-\rho_{k2}\omega_n^2\tau)\lambda+2\omega_n^2+2\rho_{k1}\omega_n^2+2\rho_{k2}\omega_n^2=0 \tag{18}$$

Fig. 2 is a stability plot using Eq. (18) under various feedback coefficients ($\rho_{k1}=1$ and $\rho_{k2}=\{0,-0.1,-0.2,-0.3,-0.4,-0.5\}$) applied to an SDOF with a period $T=2$ 2 sec with a the fundamental damping ratio $\xi=2\%$ (typical for a civil structure). Values for ρ_{k1} and ρ_{k2} were selected to meet the stability conditions from (14) and (16). Fig. 2 shows a bound on time delay for stability. This maximum time delay corresponds to $\lambda_R=0$ or $\lambda=\lambda_I i$ when the path shifts from the left half-plane to the right half-plane with varying ρ_{k2}. Substituting for λ in (10) leads to

$$-\lambda_I^2+\omega_n^2+\rho_{k1}\omega_n^2+\rho_{k2}\omega_n^2\cos(\tau\lambda_I)+(2\xi\omega_n^2\lambda_I-\rho_{k2}\omega_n^2\sin(\tau\lambda_I))i=0 \tag{19}$$

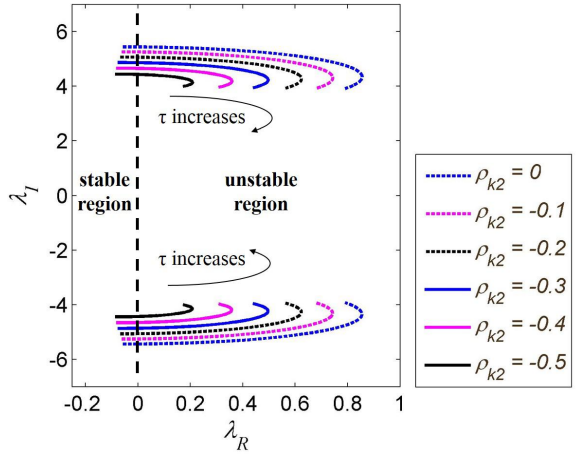

Figure 2: Stability condition of an SDOF system with a period of 2 sec and damping ratio $\xi=2\%$

Eq. (19) is satisfied when the real and imaginary terms vanish:

$$\begin{aligned}-\lambda_I^2+\omega_n^2+\rho_{k1}\omega_n^2+\rho_{k2}\omega_n^2\cos(\tau\lambda_I)&=0\\ 2\xi\omega_n^2\lambda_I-\rho_{k2}\omega_n^2\sin(\tau\lambda_I)&=0\end{aligned} \tag{20}$$

giving

$$\lambda_I^4+(4\xi^2\omega_n^2-2\omega_n^2-2\rho_{k1}\omega_n^2)\lambda_I^2+(\omega_n^2+\rho_{k1}\omega_n^2)^2-\rho_{k2}^2\omega_n^4=0 \tag{21}$$

Eq. (21) can be used to obtain a condition for stability independent of time delay. Such stability is guaranteed if the solution for λ has no imaginary parts. This occurs when

$$\rho_{k2}^2 - 4\xi^2\rho_{k1} < 4\xi^2 - 4\xi^4 \tag{22}$$

which leads to the maximum allowable time delay by solving Eqs. (20) and (21) for τ in terms of λ_I

$$\tau|_{\max} = \frac{2}{\lambda_I}\tan^{-1}\left(\frac{-2\rho_{k2}\omega_n^2 \pm \sqrt{4\rho_{k2}^2\omega_n^4 - 16\xi^2\omega_n^2\lambda_I^2}}{4\xi\omega_n\lambda_I}\right) \tag{23}$$

In summary, the study on stability led to three conditions:

1. $\rho_{k2} < 2\xi/(\omega_n\tau)$
2. $1 + \rho_{k1} + \rho_{k2} > 0$
3. $\tau|_{\max} = \frac{2}{\lambda_I}\tan^{-1}\left(\frac{-2\rho_{k2}\omega_n^2 \pm \sqrt{4\rho_{k2}^2\omega_n^4 - 16\xi^2\omega_n^2\lambda_I^2}}{4\xi\omega_n\lambda_I}\right)$

Integrating these conditions to results obtained from the H function (Fig. 1), one obtain an optimal time delay τ^* as a function of ρ. Fig. 3 plots the optimal time delay ratio ρ_{τ^*} for $\rho_{k1} = 2$ and $\rho_{k2} = -1$. The optimal time delay ratio is governed by the stability limit (red dashed line; $\rho_{\tau^*} = \tau|_{\max}/T$) until it reaches the value obtained from optimal mitigation performance (black line, $\rho_{\tau^*} = \tau^*/T$). Once the excitation ratio ρ is higher than the critical frequency ratio $\rho_{cr} = \xi + \sqrt{\xi^2 + \rho_{k1} + 1}$, no time delay (blue dashed line, $\rho_{\tau^*} = 0$) provides an optimal performance.

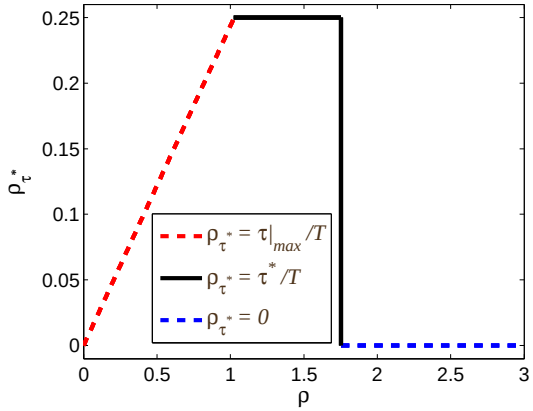

Figure 3: Optimal time delay ratio ρ_τ under different frequency input with $\rho_{k1} = 2$ and $\rho_{k2} = -1$

2.2 Optimal Time Delay - Information Theory

From the Embedding Theorem, a procedure to select τ^* is to conduct the mutual information (MI) test[37] based on Shannon's information theory. The MI test measures the amount of information contain in an observation given the past observations. Consider two sets of measurements f_1 and f_2. The MI on f_1 and f_2 is given by

$$\begin{aligned}\mathrm{MI}(f_1, f_2) = &-\sum_{i=1}^{n} \mathrm{p}(f_{1i})\log_2\mathrm{p}(f_{1i}) - \sum_{j=1}^{n}\mathrm{p}(f_{2j})\log_2\mathrm{p}(f_{2j}) \\ &+ \sum_{i=1}^{n}\sum_{j=1}^{n}\mathrm{p}(f_{1i}f_{2j})\log_2\mathrm{p}(f_{1i}f_{2j})\end{aligned} \tag{24}$$

over n measurements. The first local minima of MI is used to select τ^*. There exists an analytical solution for τ^* using the MI test for a harmonic excitation, as derived in Reference[38] for a discretized signal. Consider two signals $f_1(t)$ and $f_2(t)$ that consist of two sinusoidal functions with a phase shift angle $\phi \in [0, 2\pi]$.

$$\begin{aligned} f_1 &= \hat{f}_1 \sin(\theta) \\ f_2 &= \hat{f}_2 \sin(\theta + \phi) \end{aligned} \tag{25}$$

where θ is uniformly distributed over $[-\pi, \pi]$ and can be taken as $\theta = \Omega t$. The $\mathrm{MI}(f_1, f_2)$ is given by

$$\begin{aligned} \mathrm{MI}(f_1, f_2) &= (N-1) + \log_2(\frac{\pi \hat{f}_2}{2}) - J(f_2|f_1) \\ J(f_2|f_1) &= \int_{-\hat{f}_1}^{\hat{f}_1} \frac{1}{\pi\sqrt{\hat{f}_1^2 - \alpha^2}} J(\mathrm{p}_\alpha) d\alpha \end{aligned} \tag{26}$$

where N is the length of the discretized signals, $J(\mathrm{p}_\alpha)$ is the discrete entropy and p_α is the discrete probability for a particular value α in f_1. The discrete entropy $J(\mathrm{p}_\alpha)$ and probability p_α are given by

$$\begin{aligned} J(\mathrm{p}_\alpha) &= -\mathrm{p}_\alpha \log_2(\mathrm{p}_\alpha) - (1 - \mathrm{p}_\alpha)\log_2(1 - \mathrm{p}_\alpha) \\ \mathrm{p}_\alpha &= \frac{D_1}{D_1 + D_2} \end{aligned} \tag{27}$$

where D_1 and D_2 are defined by

$$\begin{aligned} D_1 &= \sqrt{\cos^2\phi + \frac{2\alpha}{\hat{f}_1}\sqrt{1 - (\frac{\alpha}{\hat{f}_1})^2}\sin\phi\cos\phi - (\frac{\alpha}{\hat{f}_1})^2\cos 2\phi} \\ D_2 &= \sqrt{\cos^2\phi - \frac{2\alpha}{\hat{f}_1}\sqrt{1 - (\frac{\alpha}{\hat{f}_1})^2}\sin\phi\cos\phi - (\frac{\alpha}{\hat{f}_1})^2\cos 2\phi} \end{aligned} \tag{28}$$

Since N and $\hat{f}_2$ are constants, the first local minima of $\mathrm{MI}(f_1, f_2)$ occurs when the discrete entropy $J(\mathrm{p}_\alpha)$ reaches its maximum value $J(\mathrm{p}_\alpha) = 1$. It leads to the probability $\mathrm{p}_\alpha = 1/2$ and the optimal phase shift ϕ_{opt}

$$\phi_{\mathrm{opt}} = \pm\frac{\pi}{2} \tag{29}$$

This is equivalent to a quarter of the excitation period 2π, or

$$\tau^* = 0.25T \tag{30}$$

This solution is in agreement with the optimal value obtained from the analytical solution of the equation of motion presented in the last subsection.

3. ISDC ALGORITHM

The comparison of analytical solutions in the previous section demonstrates that the MI test can be used to select τ^*. However, limitations in the online application of this strategy are the inability to satisfy the stability condition $\tau|_{\max}$, and the sub-optimal performance for $\rho > \rho_{cr}$ as ρ_{cr} is assumed to be unknown. A solution is to allow the control gains $\mathbf{K}$ to be adaptive in order to ensure stability and provide a better control performance for cases where $\rho > \rho_{cr}$. The adaptive rule on the control gains is derived in what follows, and the subsequent subsection presents the sequential adaptive algorithm used for the ISDC.

3.1 Adaptive Control Gains

The adaptive control gains follow a back-propagation rule. Its stability can be shown using Lyapunov theory. Here, the state-space representation is adopted to facilitate the application to multi-degree-of-freedom systems. The state-space representation of Eq. (2) is written

$$\dot{\mathbf{X}} = \mathbf{A}\mathbf{X} + \mathbf{B}_f f + \mathbf{B}_u u \tag{31}$$

where $\mathbf{X} = \begin{bmatrix} x & \dot{x} \end{bmatrix}^T \in \mathbb{R}^{2\times 1}$ is state vector and $u = \mathbf{K}^T \nu$ is control input (Eq. (1)) where $\mathbf{K} \in \mathbb{R}^{2\times 1}$ is adaptive, with

$$\mathbf{A} = \begin{bmatrix} 0 & 1 \\ -\frac{k}{m} & -\frac{c}{m} \end{bmatrix}_{2\times 2} \qquad \mathbf{B}_f = \mathbf{B}_u = \begin{bmatrix} 0 \\ -\frac{1}{m} \end{bmatrix}_{2\times 1}$$

Take the following sliding surface s[39]

$$s = \Lambda \mathbf{e} = \Lambda(\mathbf{X} - \mathbf{X}_d) = \Lambda \mathbf{X} \tag{32}$$

where $\Lambda = \begin{bmatrix} \lambda & 1 \end{bmatrix} \in \mathbb{R}^{1\times 2}$ is a user-defined weight matrix with p being a strictly positive constant, e is the error between the actual state $\mathbf{X}$ and the desired state $\mathbf{X}_d$ taken as $\mathbf{X}_d = \mathbf{0}$. Consider the following Lyapunov function V

$$V = \frac{1}{2}[s^2 + \tilde{\mathbf{K}}^{\mathbf{T}} \Gamma^{-1} \tilde{\mathbf{K}}] \tag{33}$$

where $\Gamma = \gamma \mathbf{I}$ is positive definite diagonal matrix with equal weights γ representing the adaptation weights, and the tilde denotes the error between the actual and desired values ($\tilde{\mathbf{K}} = \mathbf{K} - \mathbf{K}_d; \tilde{\nu} = \nu - \nu_d$, with subscript d denoting the desired value). Consider the time derivative $\dot{V}$

$$\begin{aligned} \dot{V} &= s\dot{s} + \tilde{\mathbf{K}}^T \Gamma^{-1} \dot{\tilde{\mathbf{K}}} \\ &= s\Lambda(\mathbf{A}\mathbf{e} + \mathbf{B}_u(\mathbf{K}^T \nu - \mathbf{K}_d^T \nu_d)) + \tilde{\mathbf{K}}^T \Gamma^{-1} \dot{\tilde{\mathbf{K}}} \\ &= s\Lambda(\mathbf{A}\mathbf{e} + \mathbf{B}_u(\tilde{\mathbf{K}}^T \nu + \mathbf{K}_d^T \nu - \mathbf{K}_d^T \nu_d)) + \tilde{\mathbf{K}}^T \Gamma^{-1} \dot{\tilde{\mathbf{K}}} \\ &= \mathbf{e}^T \Lambda^T \Lambda \mathbf{A}\mathbf{e} + \tilde{\mathbf{K}}^T \nu \Lambda \mathbf{B}_u s + \tilde{\mathbf{K}}^T \Gamma^{-1} \dot{\tilde{\mathbf{K}}} + s\Lambda \mathbf{B}_u \mathbf{K}_d^T \tilde{\nu} \\ &= \mathbf{e}^T \Lambda^T \Lambda \mathbf{A}\mathbf{e} + \tilde{\mathbf{K}}^T (\nu \Lambda \mathbf{B}_u s + \Gamma^{-1} \dot{\mathbf{K}}) + s\Lambda \mathbf{B}_u \mathbf{K}_d^T \tilde{\nu} \end{aligned} \tag{34}$$

The first term in Equation (34) is negative definite for $\mathbf{A}$ negative definite, which is the case for applications to civil structures.[7] The delay vector ν is determined by the MI test, and it is assumed that it will converge to $\tilde{\nu}_d$ ($\tilde{\nu} \approx \mathbf{0}$), making the last term approximately 0.

$$\dot{\mathbf{K}} = -\Gamma \nu \text{sgn}(\Lambda \mathbf{B}_u) s \tag{35}$$

where sgn is the sign or signum function

$$\text{sgn}(\Lambda \mathbf{B_u}) = \begin{cases} -1 & \text{if} \quad \Lambda \mathbf{B}_u < 0 \\ 0 & \text{if} \quad \Lambda \mathbf{B}_u = 0 \\ 1 & \text{if} \quad \Lambda \mathbf{B}_u > 0 \end{cases} \tag{36}$$

The adaptive rule (Eq. (35)) can be written in a discrete form:

$$\mathbf{K}(t) = \mathbf{K}(t-1) - \Delta_t \Gamma \nu \text{sgn}(\Lambda \mathbf{B}_u) s \tag{37}$$

3.2 Sequential Adaptive ISDC

The ISDC consists of sequentially selecting τ^* using the last n observations, and adapting τ using

$$\tau(t) = \tau(t-1) + \Delta_t \cdot \text{sgn}(\tau^* - \tau(t-1)) \tag{38}$$

It follows from Eq. (38) that $\tau(t-1)$ can only be incremented or decremented by a unit sampling rate at each time step. Such adaptation rule is used to ensure stability as $y(\tau) \approx y(\tau \pm \Delta_t)$. The sequential application of the ISDC is described in Algorithm 1.

Algorithm 1: Sequential adaptation algorithm for the ISDC

Input: $\{ \quad [y(t) \quad y(t-1) \quad y(t-2) \quad \ldots \quad y(t-n+1)]^T \quad \tau(t-1) \quad n \quad \Delta_t \quad \mathbf{K}(t-1) \quad \}$
Output: $u(t)$

1 Calculate the state error **e** based on the observation $y(t)$
2 Compute the probabilities p(·) based on the last n observations (Eq. (24))
3 Find τ^* by conducting the MI test (Eq. (24))
4 Adapt τ usinng Eq. (38)
5 Contruct ν
6 Adapt **K** using Eq. (37)
7 Compute the output $u(t) = \mathbf{K}^T(t)\nu(t)$

While Algorithm 1 is designed to be applied in real-time, step 2 can utilize significant computation time, which will depend on the number of discrete bins MI_{bin} used in computing p(·), and the search space (number of possible τ). In previous works,[7] the authors showed that the MI test could be applied in real-time provided that the search space was limited over $\tau(t-1) \pm \Delta_t$ for n not unrealistically large. Such condition on the search space seems realistic given the adaptation limits on τ at every time step. However, further investigations showed possible chattering in the MI function, which could lead to the erroneous identification of a local minima. Here, the MI test is conducted over a larger space and the function smoothen. Such strategy requires larger computation time and impedes real-time applicability. Real-time application of the ISDC will require more investigation and is part of future work.

4. NUMERICAL SIMULATIONS

This section conducts numerical simulations to demonstrate the performance of the proposed ISDC. First, the controller is applied on an SDOF subjected to harmonic excitation. It is followed by two short examples used to show the promise of the ISDC at multi-hazard excitations. These excitations include a multi-frequencies period excitation, and an impulse load, both applied to the same SDOF system.

4.1 SDOF - Harmonic Excitation

The first set of simulations consists of subjecting an SDOF to a harmonic excitation $f(t) = \hat{f}\sin(\Omega t)$. The system's parameters are listed in Table 1. Two different excitations are considered: 1) $\Omega = 0.5\omega_n$, which is a frequency located in the unstable zone for $\rho_\tau = 0.25$; and 2) $\Omega = 2\omega_n$, which is a zone of sub-optimal performance for $\rho_\tau = 0.25$. The control objective is displacement reduction. It is used to assess the performance of the ISDC. Four control cases are considered:

1. The proposed ISDC (Algorithm 1)
2. Fixed gain & adaptive delay: Control gains $\rho_{k1} = 2$ and $\rho_{k2} = -1$ are selected (the same gains as used to create Fig. 1). The time delay is selected and adapted as per the Algorithm 1.
3. Adaptive gain & fixed delay: Control gains are adapted as per Algorithm 1. The time delay is selected from Fig. 3.
4. Fixed gain & fixed delay: Control gains $\rho_{k1} = 2$ and $\rho_{k2} = -1$ are selected, and the time delay is selected from Fig. 3.

The maximum control force is bounded by $u_{\max}$ = 2 kN for each control case.

Table 1: Simulation parameters

object	parameter class	parameter	value
model	mass	m	0.05 kg
	stiffness	k	2 kN/m
	damping ratio	ξ	2%
	natural period	T	1 s
input	maximum force	$u_{\max}$	2 kN
	amplitude of excitation	$\hat{f}$	2 kN
	initial gain value	$k_1(t=0)$	4 kN/m
	initial gain value	$k_2(t=0)$	-2 kN/m
	sampling rate	Δ_t	0.01 s
	observation size	n	100
	discrete bin number	$\mathrm{MI}_{\mathrm{bin}}$	40
adaptation	weight	λ	1
	weight	γ_k	1

Simulation results are shown in Fig. 4. A comparison of the time series (Figs. 4(a) and (b)) shows that the ISDC (thick red line) stabilizes the system fast than the three other control alternatives. A study of the control forces for $\Omega = 0.5\omega_n$ (Fig. 4(c)) shows more chattering in the control force computed by the ISDC and saturation at $u_{\max}$, where saturation only occurs over the first 2 sec for the other controllers. For $\Omega = 2\omega_n$, all controllers saturate, and the ISDC outputs similar forces for a significantly higher displacement mitigation. Figs. 4(e) and (f) are plots of the evolution of ρ_τ. The time delays do not converge rapidly to ρ_τ = 0.25 in the case $\Omega = 0.5\omega_n$, which is responsible for the stability of the system under the fixed gain & adaptive delay case. The time delays converge rapidly to ρ_τ = 0.25 in the case $\Omega = 2\omega_n$, as expected.

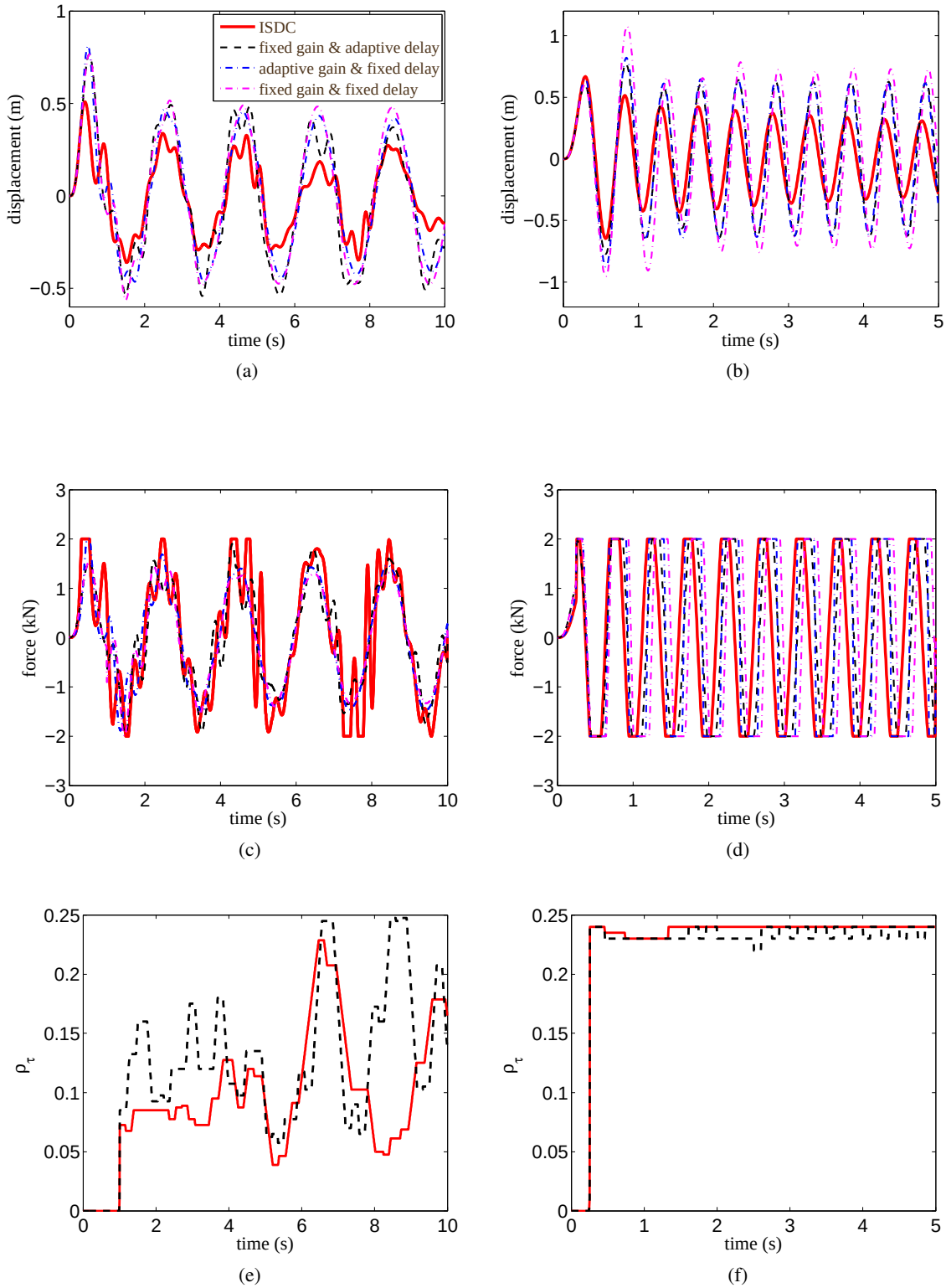

Figure 4: Time series displacement response : (a) $\Omega = 0.5\omega_n$; and (b) $\Omega = 2\omega_n$. Time series control force: (c) $\Omega = 0.5\omega_n$; and (d) $\Omega = 2\omega_n$. Time series time delay : (e) $\Omega = 0.5\omega_n$; and (f) $\Omega = 2\omega_n$.

4.2 Multi-Hazards

Two different multi-hazard excitations are simulated in order to demonstrate the promise of the ISDC at mitigating excitations of different dynamics. They are simulated on the same SDOF used in the previous section (Table 1). The first one is a period excitation of the type $f(t) = \hat{f}(\sin(\Omega t) + \sin(2\Omega t))$ with $\Omega_1 = 0.5\omega_n$ and $\Omega_2 = 2\omega_n$ (two distinct cases). The second one is an impulse excitation, simplified by imposing an initial condition on the velocity of the system: $\dot{x}(0) = 10$ m/s. Three control cases are compared:

1. The proposed ISDC (Algorithm 1)
2. No time delay control (NDC): A negative displacement feedback $u(t) = -\rho_k k x(t)$, with the arbitrary gain $\rho_k = 1$.
3. Linear quadratic regulator control (LQR): An LQR controller optimized to provide the best control performance.

As before, the maximum control force is bounded by $u_{\max} = 2$ kN for each control case.

Fig. 5 shows the result from the periodic excitation. Results are similar to the single-harmonic case discussed above. The ISDC is capable of good mitigation performance. It the case of $\Omega_1 = 0.5\omega_n$, displacement mitigation is close to the one provided by the LQR. The LQR performs significantly better for the case $\Omega_2 = 2\omega_n$, as one would expect given the system's knowledge utilized in constructing the LQR rule. The evolution of the time delay (Figs. 5(e) and (f)) are shown for τ instead of ρ_τ given the multi-frequency response of the system. The evolution of the time delay is similar to the one from the single-harmonic case, except for τ converging to a lower value after 4.5 sec for the case $\Omega_2 = 2\omega_n$.

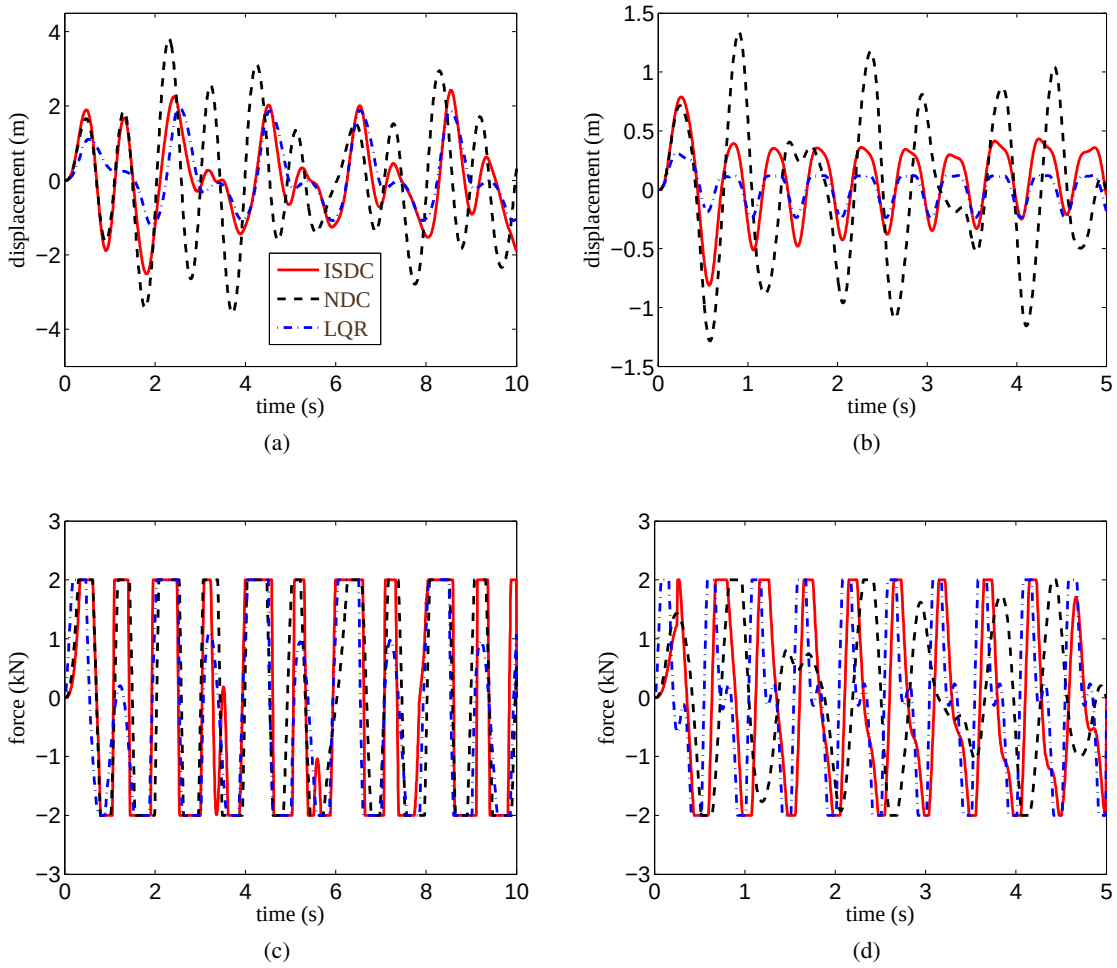

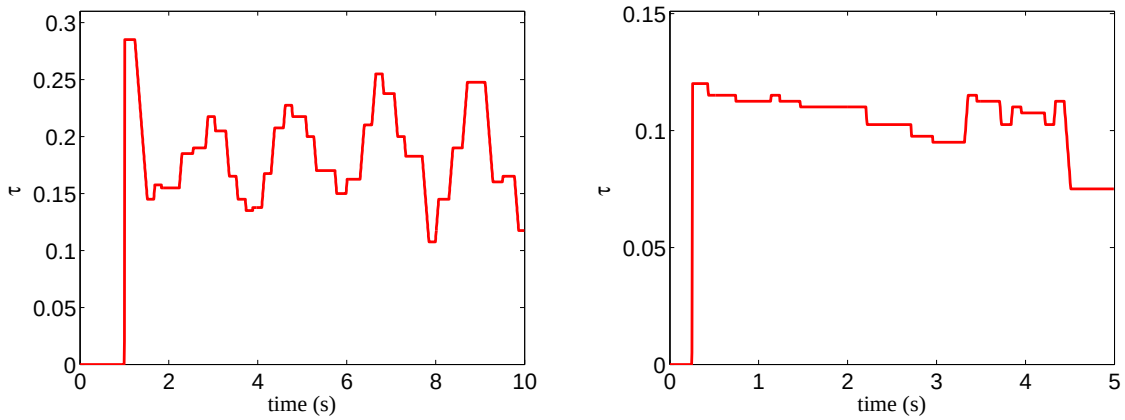

(e) (f)

Figure 5: Time series displacement response : (a) $\Omega = 0.5\omega_n$; and (b) $\Omega = 2\omega_n$. Time series control force: (c) $\Omega = 0.5\omega_n$; and (d) $\Omega = 2\omega_n$. Time series time delay : (e) $\Omega = 0.5\omega_n$; and (f) $\Omega = 2\omega_n$.

Fig. 6 shows the results for the impulse load. Results show that the stabilization performance of the ISDC is similar to the LQR's, while the NDC was not successful at quickly stabilizing the system, which can be explained by the lag present in a displacement-based control rule applied to a system subjected to an initial velocity. The time delay (Fig. 6(c)) converges to a stable value.

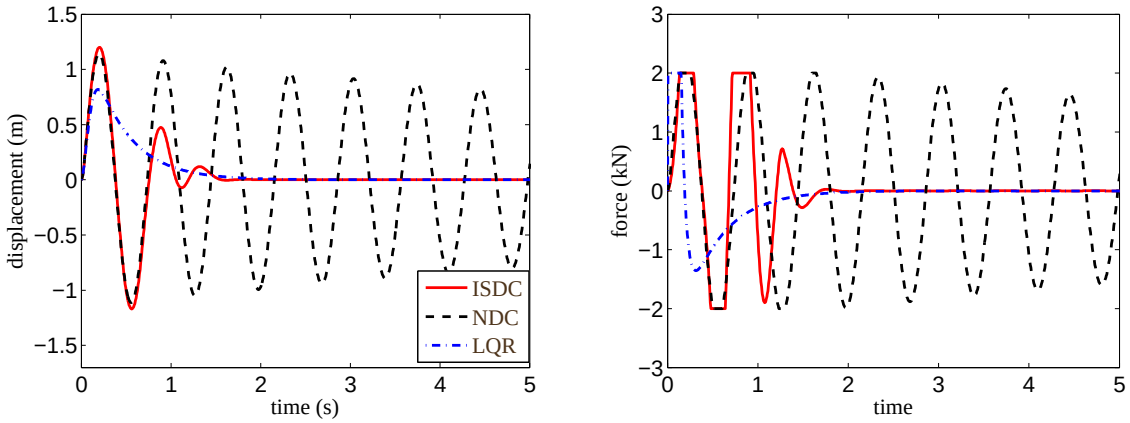

(a) (b)

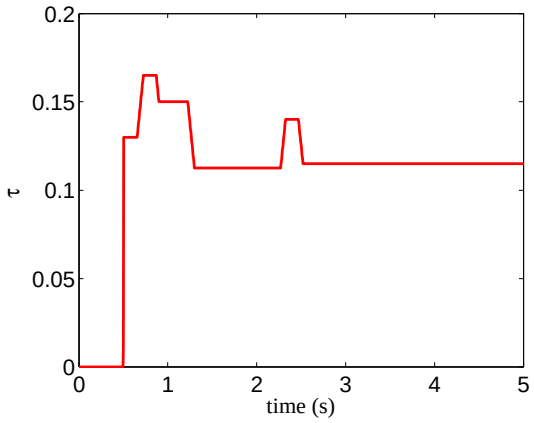

(c)

Figure 6: Time series measurements: (a) displacement response ; (b) control force; and (c) time delay.

5. CONCLUSION

In this paper, a new type of time-delay controller was introduced termed input-space dependent controller (ISDC). The ISDC is a data-based controller, which was designed to adapt the control rule's time delay and embedding dimension based on the last few observations. It is therefore adaptable to new sets of inputs with different dynamic signatures, and can be used in the context where systems are uncertain and excitations are unknown. The ISDC is therefore an ideal candidate for multi-hazard mitigation of civil structures.

The study on the ISDC was focused on the selection of the varying time delay. The algorithm consists of selecting an optimal time delay from the mutual information (MI) test using the last few observations. Such strategy is based on the Embedding Theorem, and its applicability was demonstrated by comparing the analytical solution from the MI test to the analytical solution of a single-degree-of-freedom system subjected to a harmonic excitation. In order to ensure stability, the control gains were allowed to be time varying. Their adaptation rule is a back-propagation rule.

Numerical simulations were conducted to demonstrate the performance of the ISDC. The first set of simulations consisted of a single harmonic excitation to validate the algorithm itself. Results showed that the adaptability of both the control gains and the time delay provided significantly better mitigation performance when compared with any permutation involving fixed parameters. The second set of simulations consisted of a multi-harmonic excitation and an impulse-type load to show the promise of the algorithm at multi-hazard mitigation. The ISDC was compared against an optimal controller designed using full knowledge of the structure: a linear quadratic regulator (LQR). While the LQR always outperformed the ISDC, the ISDC showed mitigation performance closed to the LQR's in most cases.

It follows that the ISDC is a promising data-based solution for mitigating structures subjected to diverse types of natural and man-made hazards, because it is 1) relying on local and limited sensors only; 2) not requiring prior evaluation or training; and 3) adapting to systems nonstationarities. Future work includes the design of a time varying embedding dimension, and real-time applicability of the methodology.

ACKNOWLEDGMENT

This material is based upon work supported by the National Science Foundation under Grant No. 1300960. Their support is gratefully acknowledged. Any opinions, findings, and conclusions or recommendations expressed in this material are those of the authors and do not necessarily reflect the views of the National Science Foundation.

REFERENCES

[1] Ubertini, F., "Active feedback control for cable vibrations," *Smart Structures and Systems* **4**(4), 407–428 (2008).

[2] Venanzi, I., Ubertini, F., and Materazzi, A. L., "Optimal design of an array of active tuned mass dampers for wind-exposed high-rise buildings," *Structural Control and Health Monitoring* **20**(6), 903–917 (2013).

[3] Cao, L., Downey, A., Laflamme, S., Taylor, D., and Ricles, J., "Variable friction device for structural control based on duo-servo vehicle brake: Modeling and experimental validation," *Journal of Sound and Vibration* **348**, 41–56 (2015).
[4] Yang, J. N. and Agrawal, A. K., "Semi-active hybrid control systems for nonlinear buildings against near-field earthquakes," *Engineering Structures* **24**(3), 271–280 (2002).
[5] He, W., Agrawal, A., and Yang, J., "Novel semiactive friction controller for linear structures against earthquakes," *Journal of Structural Engineering* **129**(7), 941–950 (2003).
[6] Connor, J. J. and Laflamme, S., [*Structural Motion Engineering*], Springer (2014).
[7] Laflamme, S., Slotine, J., and Connor, J., "Self-organizing input space for control of structures," *Smart Materials and Structures* **(in press)** (2012).
[8] Zou, Z., Bao, Y., Li, H., Spencer, B. F., and Ou, J., "Embedding compressive sensing-based data loss recovery algorithm into wireless smart sensors for structural health monitoring," *Sensors Journal, IEEE* **15**(2), 797–808 (2015).
[9] Anderson, B. D. et al., "Failures of adaptive control theory and their resolution," *Communications in Information & Systems* **5**(1), 1–20 (2005).
[10] Anderson, B. D. and Dehghani, A., "Challenges of adaptive control–past, permanent and future," *Annual reviews in control* **32**(2), 123–135 (2008).
[11] Hou, Z.-S. and Wang, Z., "From model-based control to data-driven control: Survey, classification and perspective," *Information Sciences* **235**, 3–35 (2013).
[12] Lee, H.-J., Yang, G., Jung, H.-J., Spencer, B. F., and Lee, I.-W., "Semi-active neurocontrol of a base-isolated benchmark structure," *Structural Control and Health Monitoring* **13**(2-3), 682–692 (2006).
[13] Laflamme, S. and Connor, J., "Application of self-tuning Gaussian networks for control of civil structures equipped with magnetorheological dampers," in [*Proceedings of SPIE*], **7288**, 72880M (2009).
[14] Laflamme, S., Slotine, J.-J. E., and Connor, J. J., "Wavelet network for semi-active control," *Journal of Engineering Mechanics* (2011).
[15] Hou, Z. and Jin, S., "Data-driven model-free adaptive control for a class of mimo nonlinear discrete-time systems," *Neural Networks, IEEE Transactions on* **22**(12), 2173–2188 (2011).
[16] Spall, J. C., "Feedback and weighting mechanisms for improving jacobian estimates in the adaptive simultaneous perturbation algorithm," *Automatic Control, IEEE Transactions on* **54**(6), 1216–1229 (2009).
[17] Van Helvoort, J., de Jager, B., and Steinbuch, M., "Direct data-driven recursive controller unfalsification with analytic update," *Automatica* **43**(12), 2034–2046 (2007).
[18] Campestrini, L., Eckhard, D., Gevers, M., and Bazanella, A. S., "Virtual reference feedback tuning for non-minimum phase plants," *Automatica* **47**(8), 1778–1784 (2011).
[19] Li, H., Liu, H., Gao, H., and Shi, P., "Reliable fuzzy control for active suspension systems with actuator delay and fault," *Fuzzy Systems, IEEE Transactions on* **20**(2), 342–357 (2012).
[20] Pyragas, K., "Continuous control of chaos by self-controlling feedback," *Physics letters A* **170**(6), 421–428 (1992).
[21] Socolar, J. E., Sukow, D. W., and Gauthier, D. J., "Stabilizing unstable periodic orbits in fast dynamical systems," *Physical Review E* **50**(4), 3245 (1994).
[22] Ahlborn, A. and Parlitz, U., "Stabilizing unstable steady states using multiple delay feedback control," *Physical review letters* **93**(26), 264101 (2004).
[23] Gjurchinovski, A. and Urumov, V., "Stabilization of unstable steady states by variable-delay feedback control," *EPL (Europhysics Letters)* **84**(4), 40013 (2008).
[24] Gjurchinovski, A. and Urumov, V., "Variable-delay feedback control of unstable steady states in retarded time-delayed systems," *Physical Review E* **81**(1), 016209 (2010).
[25] Takens, F., [*Detecting strange attractors in turbulence*], Springer (1981).
[26] Stark, J., "Delay embeddings for forced systems. I. Deterministic forcing," *Journal of Nonlinear Science* **9**(3), 255–332 (1999).
[27] Stark, J., Broomhead, D., Davies, M., and Huke, J., "Delay embeddings for forced systems. II. Stochastic forcing," *Journal of Nonlinear Science* **13**(6), 519–577 (2003).
[28] Caballero, V., "On an embedding theorem," *Acta Mathematica Hungarica* **88**(4), 269–278 (2000).
[29] Monroig, E., Aihara, K., and Fujino, Y., "Modeling dynamics from only output data," *Physical Review E* **79**(5), 56208 (2009).

[30] Moniz, L., Nichols, J., Nichols, C., Seaver, M., Trickey, S., Todd, M., Pecora, L., and Virgin, L., "A multivariate, attractor-based approach to structural health monitoring," *Journal of Sound and Vibration* **283**(1-2), 295–310 (2005).

[31] Overbey, L., Olson, C., and Todd, M., "A parametric investigation of state-space-based prediction error methods with stochastic excitation for structural health monitoring," *Smart Materials and Structures* **16**, 1621–1638 (2007).

[32] Li, K. and Peng, J., "Neural input selection–A fast model-based approach," *Neurocomputing* **70**(4-6), 762–769 (2007).

[33] da Silva, A., Alexandre, P., Ferreira, V., and Velasquez, R., "Input space to neural network based load forecasters," *International Journal of Forecasting* **24**(4), 616–629 (2008).

[34] Tikka, J., "Simultaneous input variable and basis function selection for RBF networks," *Neurocomputing* **72**(10-12), 2649–2658 (2009).

[35] Zolock, J. and Greif, R., "A Methodology for the Modeling of Forced Dynamical Systems From Time Series Measurements Using Time-Delay Neural Networks," *Journal of Vibration and Acoustics* **131**, 011003 (2009).

[36] Kennel, M. B., Brown, R., and Abarbanel, H. D., "Determining embedding dimension for phase-space reconstruction using a geometrical construction," *Physical review A* **45**(6), 3403 (1992).

[37] Fraser, A. M. and Swinney, H. L., "Independent coordinates for strange attractors from mutual information," *Physical review A* **33**(2), 1134 (1986).

[38] Michalowicz, J. V., Nichols, J. M., and Bucholtz, F., "Calculation of entropy and mutual information for sinusoids," tech. rep., DTIC Document (2009).

[39] Slotine, J.-J. E., Li, W., et al., [*Applied nonlinear control*], vol. 199, Prentice-hall Englewood Cliffs, NJ (1991).